Experimental Neurology 322 (2019) 113055

Contents lists available at ScienceDirect

Experimental Neurology

journal homepage: www.elsevier.com/locate/yexnr

Research paper

# *Zfhx3* is required for the differentiation of late born D1-type medium spiny neurons

Zhuangzhi Zhang*[,1], Song Wei[1], Heng Du, Zihao Su, Yan Wen, Zicong Shang, Xiaolei Song, Zhejun Xu, Yan You, Zhengang Yang*

*State Key Laboratory of Medical Neurobiology, Institutes of Brain Science, MOE Frontier Research Center for Brain Science, Department of Neurology, Zhongshan Hospital, Fudan University, 138 Yi Xue Yuan Road, Shanghai 200032, PR China*

ARTICLE INFO

*Keywords:*
*Zfhx3*
DRD1
DRD2
Differentiation
LGE
Striatum
Medium spiny neuron
Mice

ABSTRACT

The striatum, the major component of the basal ganglia, consists of the caudate-putamen, nucleus accumbens and olfactory tubercle. The striatal principal projection neurons are comprised of medium spiny neurons (MSNs) with two dopamine receptors: DRD1 (D1 MSNs) and DRD2 (D2 MSNs). In the present study, we demonstrate that *Zfhx3* is strongly expressed in the boundary of the subventricular zone (SVZ)/mantle zone (MZ) of the lateral ganglionic eminence (LGE), and its expression in the striatum is downregulated during the first postnatal week. At the cellular level, *Zfhx3* is selectively expressed in immature D1 MSNs. In *Zfhx3* conditional knockouts, we observed an accumulation of progenitors in the LGE SVZ at E16.5 and P0, and an increase in apoptosis in the postnatal striatum. BrdU birthdating experiments revealed that late born D1 MSN production was compromised. Accordingly, we observed a significant reduction in the number of D1 MSNs, whereas the number of D2 MSNs remained unaffected in the striatum of *Zfhx3* conditional knockouts at P11. We concluded that *Zfhx3* plays a critical role in the differentiation and survival of late born D1 MSNs.

## 1. Introduction

The striatal medium spiny neurons (MSNs) can be divided into two cell types: one expresses the dopamine receptor DRD2 (D2 MSNs), which is mainly projected to the external portion of the globus pallidus and forms the indirect pathway. Another cell type specifically expresses the dopamine receptor DRD1 (D1 MSNs), which mainly projects to the internal segment of the globus pallidus and the substantia nigra pars reticulata, constituting the direct pathway (Gerfen, 1992; Gerfen et al., 1990; Gerfen and Surmeier, 2011). Keeping the balance of activity between these two pathways is deemed necessary for normal motor control (Albin et al., 1989; Gerfen and Surmeier, 2011). The striatal projection neurons are important in that their degeneration leads to the pathology observed in Huntington's disease. The cause of Parkinson's disease is also closely related to the abnormal function of basal ganglia circuits (Albin et al., 1989; DeLong, 1990; Gerfen and Surmeier, 2011). Furthermore, recent studies have shown that dysplasia or alteration of the basal ganglia pathways is a potential risk factor for neuropsychiatric disorders (obsessive-compulsive disorder/ attention deficit hyperactivity disorder) in children (Leisman and Melillo, 2013).

The lateral ganglionic eminence (LGE) includes two distinct compartments: a dorsal part, which gives rise to olfactory bulb interneurons (Li et al., 2017; Stenman et al., 2003; Waclaw et al., 2006), and a ventral part, which generates striatal projection neurons (Anderson et al., 1997; Olsson et al., 1995; Stenman et al., 2003). Recent studies showed that the transcription factors *Sp8/9* and *Six3* are necessary for the generation and differentiation of the striatal D2 MSNs (Xu et al., 2018; Zhang et al., 2016). Conversely, *Ebf1* and *Isl1* are required for the development of a subset of D1 MSNs (Ehrman et al., 2013; Garel et al., 1999; Lobo et al., 2006; Lobo et al., 2008; Lu et al., 2014). The transcription factor *Zfhx3* (formerly known as *Atbf1*), which is combined with an AT-rich element (enhancer), represses the expression of *alpha fetoprotein* (*Afp*) (Morinaga et al., 1991). In Drosophila, ZFH-2 is highly homologous with mouse ZFHX3. In the later stage of embryonic development of Drosophila, ZFH-2 is mainly expressed in the central nervous system and regulates its development by binding to the AT-rich domain upstream of the DDC gene (Lundell and Hirsh, 1992). *In vitro* studies have shown that *Zfhx3* plays an important role in the nucleus by organizing neuronal differentiation associated with cell cycle arrest (Jung et al., 2005). Recent studies showed that *Zfhx3* was highly expressed in the ganglionic eminence (Chen et al., 2017; Mayer et al., 2018). However, the roles of *Zfhx3* in LGE and striatal development still

* Corresponding authors.
*E-mail addresses:* 13210700034@fudan.edu.cn (Z. Zhang), yangz@fudan.edu.cn (Z. Yang).
[1] These authors contributed equally to this work.

https://doi.org/10.1016/j.expneurol.2019.113055
Received 8 March 2019; Received in revised form 17 June 2019; Accepted 2 September 2019
Available online 03 September 2019

remain largely unknown.

In the present study, using conditional deletion combined with RNA-Seq, RNA *in situ* hybridization and immunostaining, we show that *Zfhx3* promotes the differentiation of late born D1 MSNs. We observed an accumulation of progenitors in the LGE SVZ at E16.5 and P0. We also saw an increase in apoptosis in the postnatal striatum, and significant reductions in D1 MSNs at P11 in *Zfhx3* conditional knockout mice, whereas the number of D2 MSNs remains largely unaffected. BrdU birthdating experiments revealed that late born D1 MSN production was blocked. We concluded that *Zfhx3* plays a critical role in the differentiation and survival of late born D1 MSNs.

## 2. Materials and methods

### 2.1. Animals

*Zfhx3*$^{F/+}$ (Sun et al., 2012), *Dlx5/6-Cre-Ires-EGFP* (Stenman et al., 2003) and *Drd2-GFP* (from MMRRC) (Gong et al., 2007; Xu et al., 2018) were previously described. All mice were maintained in a mixed genetic background of C57BL/6 J and CD1. The day of vaginal plug observation was embryonic day 0.5 (E0.5), and the day of birth was considered as postnatal day 0 (P0). All animal care was approved in accordance with institutional guidelines at Fudan University, Shanghai Medical College.

### 2.2. Histology and immunohistochemistry

In this work, 20-μm thick frozen sections were used for histology and immunostaining. For histological analysis, the brain sections were consecutively immersed in different concentrations of alcohol (50%, 75%, 85%, 95% and 100%). Then, sections were counterstained with Cresyl Violet solution. Finally, they were dehydrated in 70%, 95% and 100% ethanol for 2 mins each, placed in xylenes for another 10 mins and then cover-slipped. Immunohistochemistry was performed on 20-μm thick frozen sections. Sections were rinsed with 0.05 M TBS for 10 mins, incubated in Triton-X-100 (0.5% in 0.05 M TBS) for 30 mins at room temperature (RT), and then incubated with block solution (10% donkey serum + 0.5% Triton-X-100 in 0.05 M TBS, pH = 7.2) for 2 h at RT. Primary antibodies were diluted in 10% donkey serum block solution and incubated overnight at 4 °C, then rinsed 3 times with 0.05 M TBS. Secondary antibodies (from Jackson, 1:500) matching the appropriate species were incubated for 3 h at RT. Fluorescently stained sections were then washed 3 times with 0.05 M TBS. This was followed with 4′, 6-diamidino-2-phenylindole (DAPI) (Sigma, 200 ng/ml) staining for 3 mins and sections were then cover-slipped with Gel/Mount (Biomeda, Foster City, CA). The primary antibodies used in our studies included: rat anti-BCL11b (1:1000; Abcam, ab18465, GR243609–3); rat anti-BrdU (1:150; Accurate Chemical, OBT0030s); rabbit anti-Cleaved Caspase-3 (1:500; Cell Signaling, 9661, 43); rabbit anti-DARPP-32 (1:100; Cell Signaling, 2302S, 4); guinea pig anti-DLX2 (1:2000) (Hansen et al., 2013; Kuwajima et al., 2006); rabbit anti-EBF1 (1:5000; Millipore, AB10523, 2,887,442); goat anti-EBF (1:200; Santa Cruz Biotechnology, sc-15,888); rabbit anti-FOXP1 (1:1500; Abcam, Ab16645, GR167582-2); goat anti-FOXP2 (1:500; Santa Cruz Biotechnology, sc-21,069); chicken anti-GFP (1:3000; Aves Labs, GFP-1020, GFP879484); rabbit anti-GSX2 (1:2000; Millipore, ABN162, 2,736,374); rabbit anti-ASCL1 (1:2000; Cosmo Bio, SK-T01-003, TAK3-002); rabbit anti-ATBF1 (1:3000; Medical & Biological Laboratories, D1-120, 004); mouse anti-SIX3 (1:500; Santa Cruz Biotechnology, sc-398,797, C2017) and rabbit anti-SP9 (1:500) (Zhang et al., 2016). For BrdU staining, sections were incubated in 2 N HCl for 1 h at RT, and then rinsed in 0.1 M borate buffer twice (Liu et al., 2009). Sections were washed 3 times with 0.05 M TBS, then a standard immunofluorescence protocol was used as described above. For KI67 and ZFHX3 immunostaining, sections were reactivated in 0.01 M citrate buffer (pH 6.0) at 98 °C for 5 mins. Sections were washed 3 times with 0.05 M TBS, then a standard immunofluorescence protocol was used as described above.

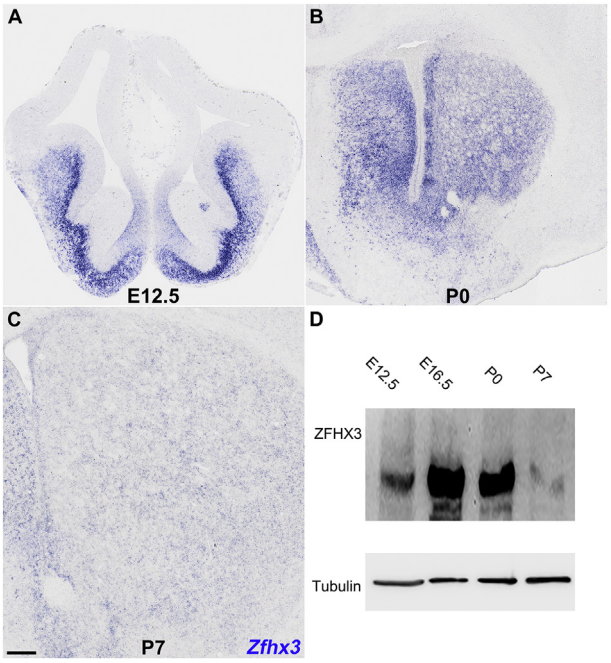


**Fig. 1.** *Zfhx3* is strongly expressed in the LGE SVZ/MZ boundary. (A-C) *Zfhx3* RNA *in situ* hybridization showed that *Zfhx3* was strongly expressed in the LGE SVZ/MZ boundary at E12.5. *Zfhx3* then spread to the whole striatum at P0. Subsequently, the expression of *Zfhx3* was dramatically decreased in the striatum at P7. (D) The expression of ZFHX3 was confirmed by western blotting. Scale bar: 200 μm in C for A-C.

### 2.3. BrdU labeling

Timed pregnant mice at E13.5 or E16.5 received a single intraperitoneal injection of bromodeoxyuridine (BrdU) (50 mg/kg body weight) and mice were sacrificed at E16.5 or P0.

### 2.4. In situ RNA hybridization

*In situ* RNA hybridization experiments were performed using digoxigenin labelled riboprobes on 20-μm frozen sections as previously described (Xu et al., 2018; Zhang et al., 2016) or made from cDNAs amplified by PCR using the following primers:

1. *Cdh8* Fwd: CTGCCACTGATGCTGACG
   *Cdh8* Rev: TTCAGGGGCGTTGTCATT
2. *Cnr1* Fwd: GTTCAAGGAGAACGAGGACAAC
   *Cnr1* Rev: CAGCAGGCAGAGCATACTACAG
3. *Cntnap3* Fwd: CTGTAATGACACCAGGAGTGGA
   *Cntnap3* Rev: AGTTTCCTCTCTGCAGAACCAG
4. *Frmd6* Fwd: ACCATTGGGAATGTCTCAGAAG
   *Frmd6* Rev: AACACTGCTATGTTCTGCCTGA
5. *Sox8* Fwd: GGAGCGACTCAGACTCTGGTACTGA

   *Sox8* Rev: TACACTTATCCAAACCGGAGAGCAA

6. *Zcchc12* Fwd: TGCAGAGGAGAGGGCAAG
   *Zcchc12* Rev: TGACAAAGAAGGCCACAACA
7. *Zfhx3* Fwd: CGATCTGGCCCAGCTCTACCA
   *Zfhx3* Rev: CTGTAAGCCTGCGAGGGCATAG
8. *Zfp521* Fwd: CAGACGCCAACAGCACAC

   *Zfp521* Rev: TGGGCCGTATCCAGATGT

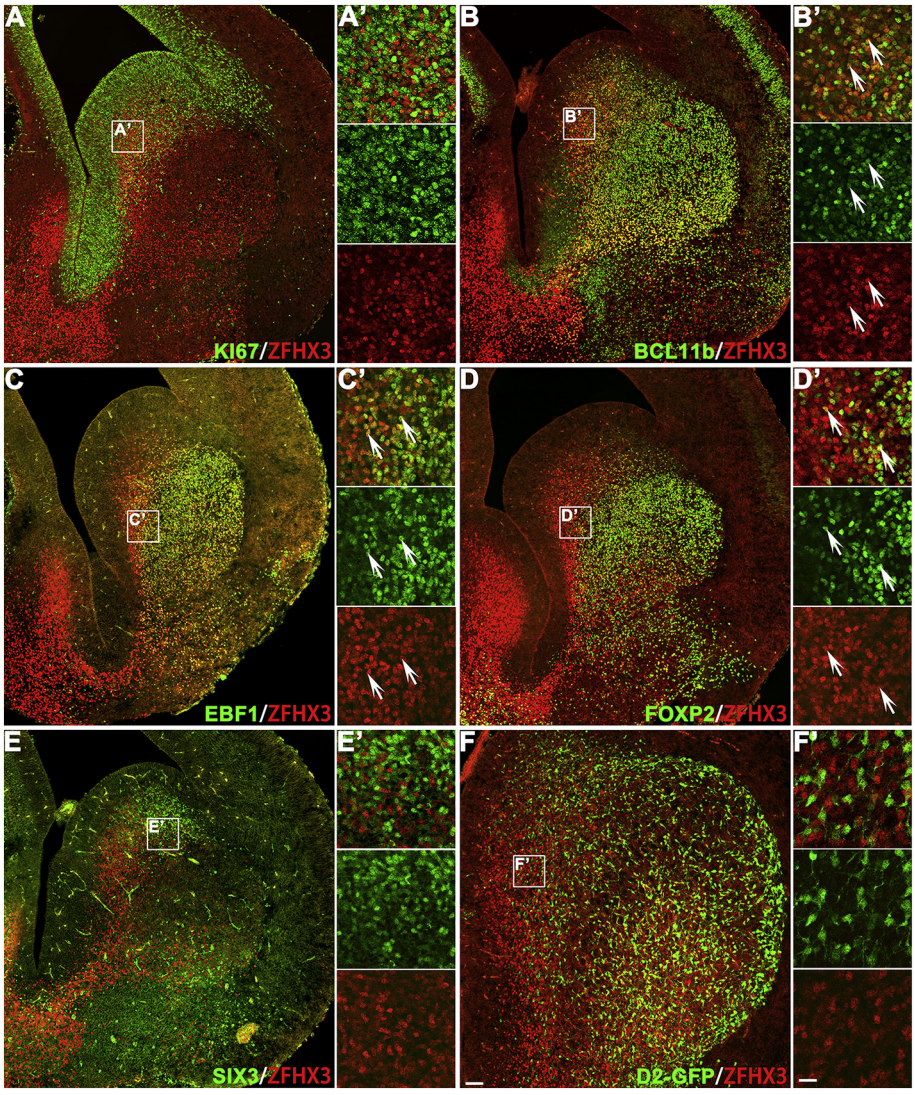


**Fig. 2.** *Zfhx3* is predominantly expressed in immature D1 MSNs.
(A-E′) Double immunostaining of ZFHX3 with different markers was performed in brain coronal sections at E15.5. (A, A′) Very few ZFHX3$^+$ cells expressed KI67. (B, B′) ZFHX3$^+$ cells were co-labelled with the striatal post-mitotic MSN marker BCL11b. (C-D′) Most EBF1$^+$ and FOXP2$^+$ cells expressed ZFHX3 in the LGE SVZ/MZ boundary. Note ZFHX3 expression began before EBF1 and FOXP2 (based on the position of the ZFHX3$^+$ cells closer to the VZ). (E, E′) None of the ZFHX3$^+$ cells expressed the D2 MSN marker SIX3. (F, F′) Double immunostaining of ZFHX3 with GFP in *Drd2-GFP* mouse brain coronal sections at E16.5. Very few ZFHX3$^+$ cells co-expressed with D2-GFP. Arrows indicate double-positive cells. Scale bar: 200 μm in F for A-F; 50 μm in F′ for A′-F′.

9. *Zfp503* Fwd: TCCCAGGGACAGACAAACTGCT

*Zfp503* Rev: TACAAGGGATCGGAGGGTTTGTT

### 2.5. Western blots

We performed Western blot analysis in wild-type mice for the expression of ZFHX3 as described elsewhere (Cobos et al., 2007).

### 2.6. Microscopy

Nissl staining, *in situ* hybridization and some fluorescent images were collected with an Olympus-BX61VS microscope using a 10× objective. Other fluorescent images were captured with an Olympus FV1000 confocal microscope system using 10×, 20× or 40× objectives. *Z*-stack confocal images were reconstructed using the FV10-ASW software. All images were merged, cropped and optimized in Photoshop CC without distorting the original information.

### 2.7. RNA sequencing (RNA-Seq) analysis

RNA-Seq analysis was performed as previously described (Li et al., 2017). The LGE (including VZ, SVZ and MZ-striatum) from E16.5 *Zfhx3-CKO* (*Dlx5/6-Cre; Zfhx3$^{F/F}$*) mice and their *Dlx5/6-Cre* or *Dlx5/6-Cre; Zfhx3$^{F/+}$* littermates (henceforth described as controls) were dissected ($n$ = 3 mice, each group). Data from this experiment have been deposited in the GEO database (GSE127976). These data have also been deposited at National Omics Data Encyclopedia (NODE), accession number (OEP000265).

### 2.8. Quantification

Nissl staining was used to define the striatal area for quantification. The striatal area was quantified using the freehand tool in ImageJ (https://imagej.net/, RRID: SCR_003070). Brain regions were identified using a mouse brain atlas and sections equivalent to the following bregma coordinates were taken (in mm): the most-rostral section, 1.18; the most-caudal section, −0.10, $n$ = 4 mice for each genotype, 8 sections per mouse).

For quantification of FOXP1$^+$ and BCL11b$^+$ cells in the mouse striatum at P11, four 20-μm thick coronal sections from rostral, intermediate, and caudal levels of the striatum were selected (n = 4 mice per group). We used the ImageJ to count the cell number of FOXP1$^+$ and BCL11b$^+$ cells in each striatum. Brain regions were identified using a mouse brain atlas and sections equivalent to the following bregma coordinates were taken (in mm): the most-rostral section, 1.18; the most-caudal section, −0.10. Data were presented as the number of FOXP1$^+$ and BCL11b$^+$ cells per section for each striatum.

For quantification of *Drd1*, *Tac1*, *Drd2* and *Penk* positive cells in the striatum at P11, four 20-μm thick coronal sections from rostral,

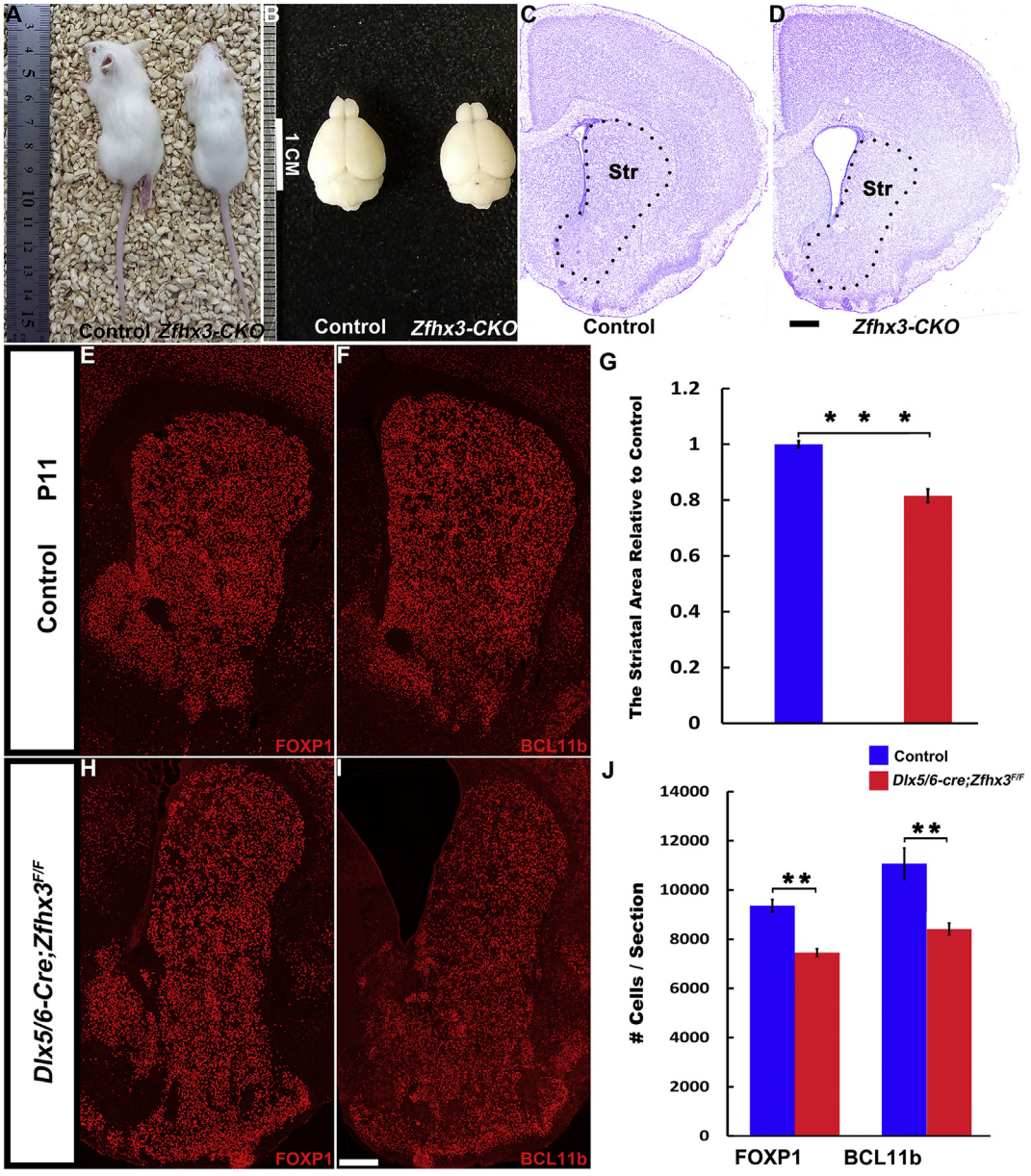


**Fig. 3.** The number of striatal MSNs is reduced in *Zfhx3-CKO* mice at P11.
(A) *Dlx5/6-Cre* control and *Zfhx3-CKO* littermates were taken at P11 to compare their sizes. (B) Images of control and *Zfhx3-CKO* mouse brains at P11. (C, D) Cresyl violet-stained coronal brain sections of control and *Zfhx3-CKO* mice at P11. Note the smaller striatum of *Zfhx3-CKO* mice compared to controls (dash lines). (E-F, H-J) Compared to controls, the numbers of FOXP1$^+$ and BCL11b$^+$ cells were reduced in *Zfhx3-CKO* mice at P11. (G) The size of mutant striatum was also reduced at P11. (Student's *t*-test, $^{**}P < .01$, $^{***}P < .001$, $n = 4$ mice per group, mean ± SEM). Str, striatum. Scale bars: 200 μm in D for C-D; 200 μm in I for E, F, H, I.

intermediate, and caudal levels of the striatum were analyzed (n = 4 mice per group). We counted all *Drd1*, *Tac1*, *Drd2* and *Penk* positive cells in the striatum. Brain regions were identified using a mouse brain atlas and sections equivalent to the following bregma coordinates were taken (in mm): the most-rostral section, 1.18; the most-caudal section, −0.10. Data were presented as the number of *Drd1*, *Tac1*, *Drd2* and *Penk* positive cells per section for each striatum.

For quantification of EBF1$^+$, FOXP1$^+$, SP9$^+$/BCL11b$^+$, GSX2$^+$ and ASCL1$^+$ cells in the LGE SVZ at E16.5, four anatomically matched 20-μm thick coronal sections spanning the rostral-caudal extent of the LGE were quantified ($n = 3$ mice per group). We counted FOXP1$^+$, EBF1$^+$, SP9$^+$/BCL11b$^+$, GSX2$^+$ and ASCL1$^+$ cells in the LGE SVZ under 10× objective. The LGE SVZ was delineated by DAPI staining. Data were presented as the number of FOXP1$^+$, EBF1$^+$, SP9$^+$/BCL11b$^+$, GSX2$^+$ and ASCL1$^+$ cells per section for each striatum.

For quantification of BrdU$^+$ cells in the striatum at E16.5 and P0, four 20-μm thick coronal sections from rostral, intermediate, and caudal levels of the LGE/striatum were analyzed (n = 3 mice per group). We counted BrdU$^+$ cells in the striatum under 10× objective. The striatum area was delineated by DAPI staining. Data were presented as the number of BrdU$^+$ cells per section for each striatum.

For quantification of Cleaved Caspase-3$^+$ cells in the striatum at P0, P3, P5, P7 and P11, four anatomically matched 20-μm thick coronal sections were assessed (n = 3 mice per group). We counted all Cleaved Caspase-3$^+$ cells in the bilateral striatum under 10× objective. The striatum area was delineated by DAPI staining. Data were presented as the number of Cleaved Caspase-3$^+$ cells per section for each striatum.

### 2.9. Statistics

Statistical significance was assessed using unpaired two-tail Student's *t*-test or one-way ANOVA followed by the Tukey-Kramer *post*

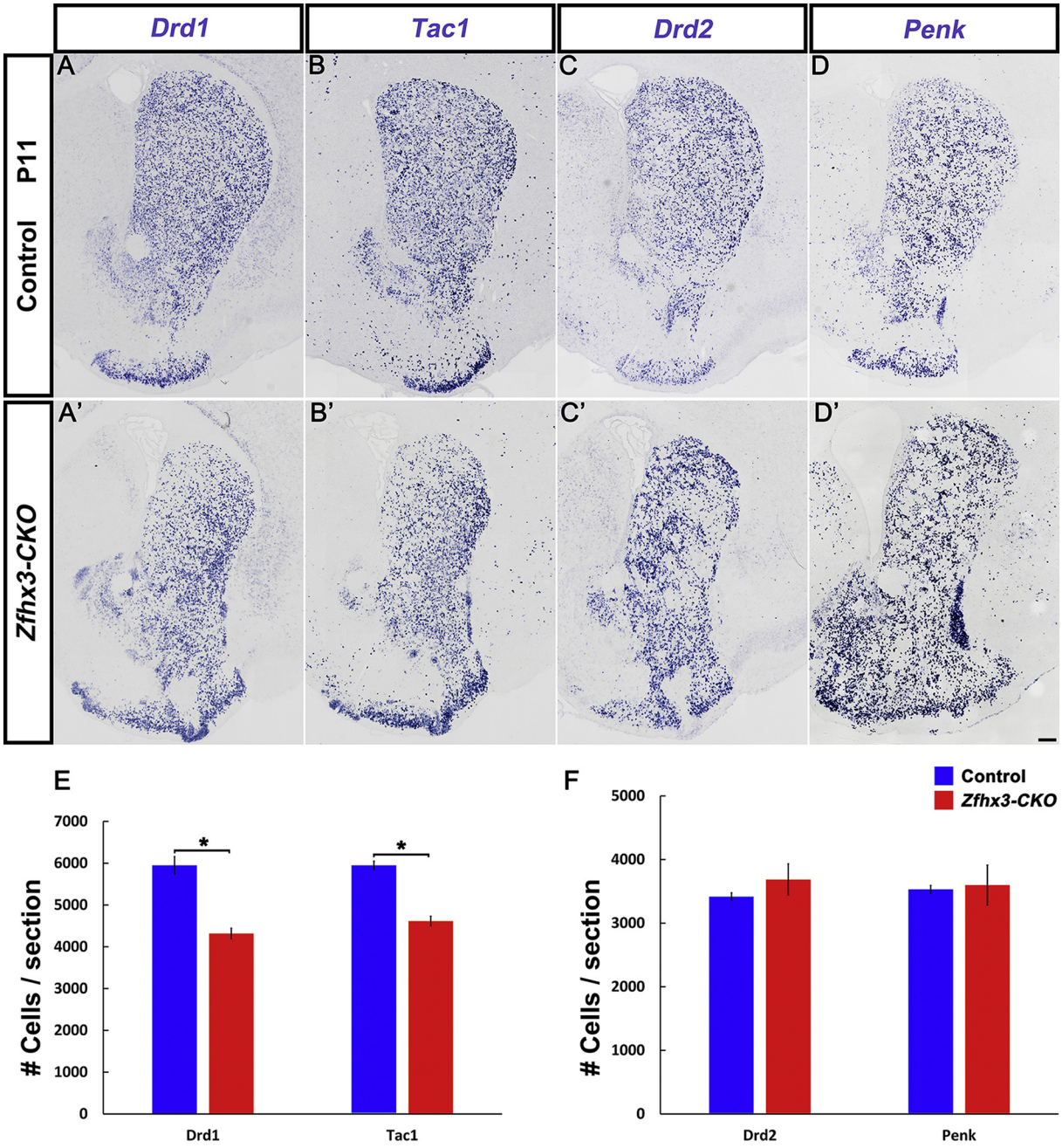


**Fig. 4.** The numbers of D1 MSNs, but not D2 MSNs are reduced in *Zfhx3-CKO*s at P11.
(A-B′) RNA *In situ* hybridization of *Drd1* and *Tac1* showed that D1 MSNs were reduced in the striatum of *Zfhx3-CKO* mice. (C-D′) *Drd2*$^+$ and *Penk*$^+$*cells* (D2 MSNs) were less affected. Note a reduction in the dorsal striatum and an enlargement of the ventral striatum in *Zfhx3-CKO* mice. (E-F) Histograms show quantification of the cell number per section for *Drd1*, *Tac1*, *Drd2* and *Penk* (Student's *t*-test, *$P < .05$, n = 4 mice per group, mean ± SEM). Scale bars: 200 μm in D′ for A-D′.

*hoc* test using SPSS 18 software. All quantification results were presented as the mean ± SEM. *P* values < .05 were considered significant.

## 3. Results

### 3.1. *Zfhx3* is strongly expressed in the LGE SVZ/MZ boundary and its expression is downregulated in the postnatal striatum

We performed *in situ* hybridization to examine the expression of *Zfhx3* mRNA at different stages during LGE/striatal development. Our results showed that *Zfhx3* was strongly expressed in the LGE SVZ/MZ boundary at E12.5 (Fig. 1A). In the LGE MZ, the *Zfhx3* expression level was lower than in the SVZ/MZ boundary (Fig. 1A). A similar expression pattern of *Zfhx3* was also observed in the LGE and/or striatum at E15.5 (Fig. 2A-E) and P0 (Fig. 1B). *Zfhx3* expression was dramatically downregulated in the striatum but remained a detectable level at P7 (Fig. 1C). The developmental expression profile of the striatal ZFHX3 protein was consistent with that of the *Zfhx3* transcripts (Fig. 1D).

### 3.2. *Zfhx3* is selectively expressed in immature D1 MSNs

D1 MSNs express the dopamine D1 receptor (DRD1) and neuropeptide TAC1 (also known as substance P), whereas D2 MSNs express the dopamine D2 receptor (DRD2) and neuropeptide enkephalin (ENK) (Gerfen, 1992; Gerfen et al., 1990; Gerfen and Surmeier, 2011). To assess whether *Zfhx3* was expressed by proliferative cells in the LGE, we

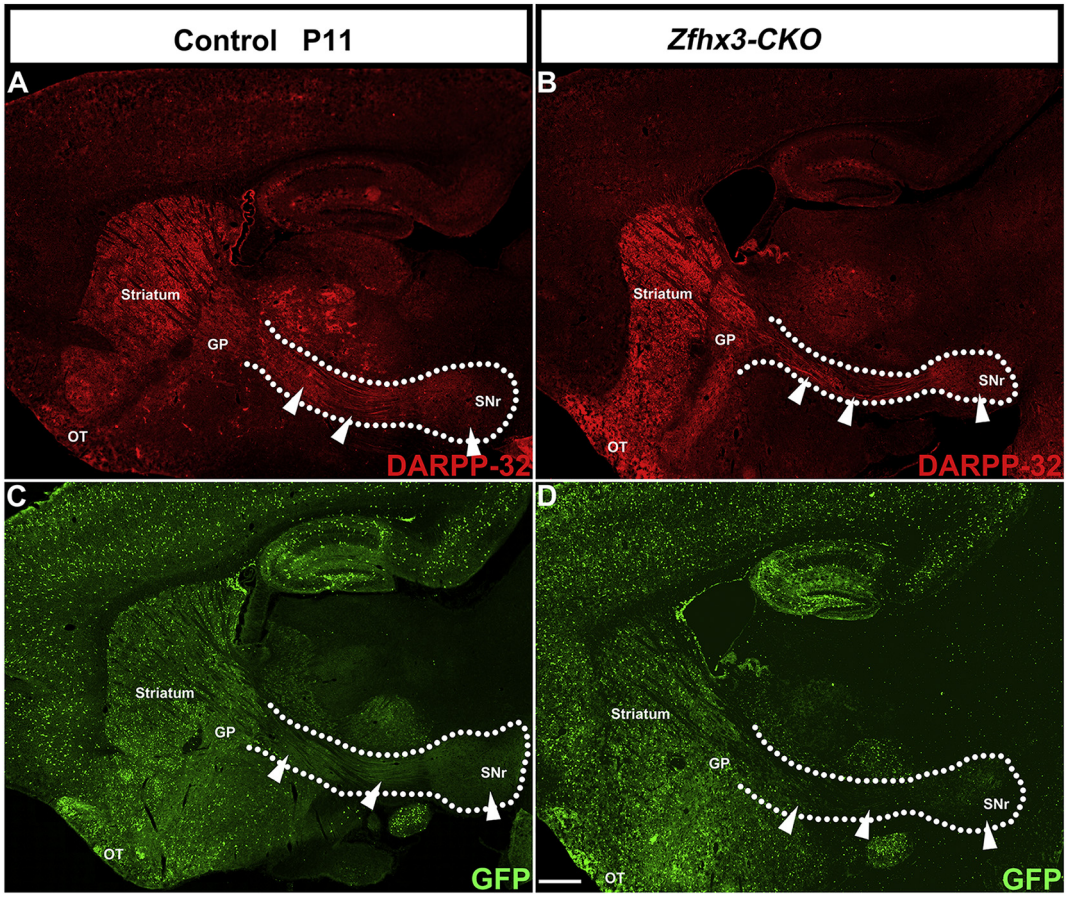


**Fig. 5.** The reduced innervation of the substantia nigra pars reticulata in *Zfhx3-CKO* mice.
(A-D) Immunostaining of DARPP-32 and GFP showed a reduction in the innervation of SNr in the *Zfhx3-CKO* mice, whereas it appeared to be normal in the GP. GP, globus pallidus; OT, olfactory tubercle; SNr, substantia nigra pars reticulata. $n$ = 3 mice per group, Scale bars: 500 μm in D for A-D.

performed double staining of ZFHX3 and the proliferative cell pan marker KI67 (Mki67) at E15.5 (Fig. 2A). Our results showed that very few ZFHX3$^+$ cells expressed KI67 (Fig. 2A′). Meanwhile, we performed double staining of ZFHX3 and the post-mitotic MSN marker BCL11b (Arlotta et al., 2008) at E15.5 (Fig. 2B). Within the LGE, most of ZFHX3$^+$ cells were co-labelled with BCL11b suggesting that ZFHX3 was predominantly expressed in early post-mitotic striatal MSNs (Fig. 2B′). Thus, it seems that when the LGE SVZ progenitor cells exit the cell cycle, they start to express *Zfhx3*. *Ebf1* and *Foxp2* have been shown to be specifically expressed in the D1 MSNs during LGE development (Lobo et al., 2006; Lobo et al., 2008; van Rhijn et al., 2018), whereas *Six3* expression is restricted to D2 MSNs (Xu et al., 2018). Double immunostaining of ZFHX3 with EBF1 or FOXP2 showed that most EBF1$^+$ cells and FOXP2$^+$ cells co-labelled with ZFHX3$^+$ cells, and *Zfhx3* expression began before *Ebf1* and *Foxp2* (based on the position of the ZFHX3$^+$ cells which were closer to the VZ) (Fig. 2C-D′). In contrast, nearly all of the ZFHX3$^+$ cells lacked expression of SIX3 (Fig. 2E, E′) at E15.5. To further confirm that *Zfhx3* was not expressed in D2 MSNs, we double immunostained ZFHX3 with GFP in *Drd2-GFP* mice at E16.5 (Fig. 2F). Our results showed that very few ZFHX3$^+$ cells were co-expressed with Drd2-GFP (Fig. 2F′). These data indicate that *Zfhx3* is specifically expressed by D1 MSNs in the striatum, providing a specific marker of D1 MSNs and suggesting that *Zfhx3* might play a role in their development.

### 3.3. LGE deletion of *Zfhx3* leads to a significant reduction in the number of D1 MSNs

To investigate whether *Zfhx3* plays a functional role in striatal MSN development, we conditionally delete *Zfhx3* expression in the LGE using *Dlx5/6-Cre* lines (*Zfhx3-CKO*). Our results showed that the weights and brain sizes of *Zfhx3-CKO* mice at P11 were reduced compared to controls (Fig. 3A, B). The most prominent phenotypes in the *Zfhx3-CKO* mouse telencephalon were atrophy and a highly disorganized striatum, shown by Nissl staining (Fig. 3C, D); the volume of the P11 mutant striatum was reduced by about 20% compared to controls (Fig. 3G). The transcription factors *Foxp1* and *Bcl11b* are expressed in all mature MSNs (Arlotta et al., 2008; Bacon et al., 2015). Compared to controls, we observed that the FOXP1$^+$ and BCL11b$^+$ cells were reduced in the *Zfhx3-CKO* striatum (Fig. 3E, F, H, I). The quantification data showed that the number of FOXP1$^+$ and BCL11b$^+$ cells was reduced by about 20% in the *Zfhx3-CKO* mice (Fig. 3J). We next performed *in situ* hybridization of the D1 MSN markers *Drd1* and *Tac1* as well as the D2 MSN markers *Drd2* and *Penk* for a detailed analysis of the function of *Zfhx3* in striatal MSNs. Compared to controls, our results showed that the expression of *Drd1* and *Tac1* mRNA was dramatically decreased in the medial part of the striatum in *Zfhx3-CKO* mice (Fig. 4A-B′). In addition, the distribution of the *Drd2* and *Penk* mRNA was also disordered (Fig. 4C-D′); these cells were mainly located in the dorsal or most ventral part (nucleus accumbens and olfactory tubercle) of the striatum. It is likely that loss of *Zfhx3* function leads to the abnormal distribution of D2 MSNs. Quantification data further revealed that the number of D1 MSNs was reduced by about 30%, whereas the number of D2 MSNs did not change (Fig. 4E-F). Because of very low proportion of MSNs that express both DRD1 and DRD2 in the striatum (Bertran-Gonzalez et al., 2008; Oude Ophuis et al., 2014; Perreault et al., 2012; Perreault et al., 2010), our above results suggest that the number of DRD1/DRD2 double positive cells was largely unaffected in the *Zfhx3-CKO* mice.

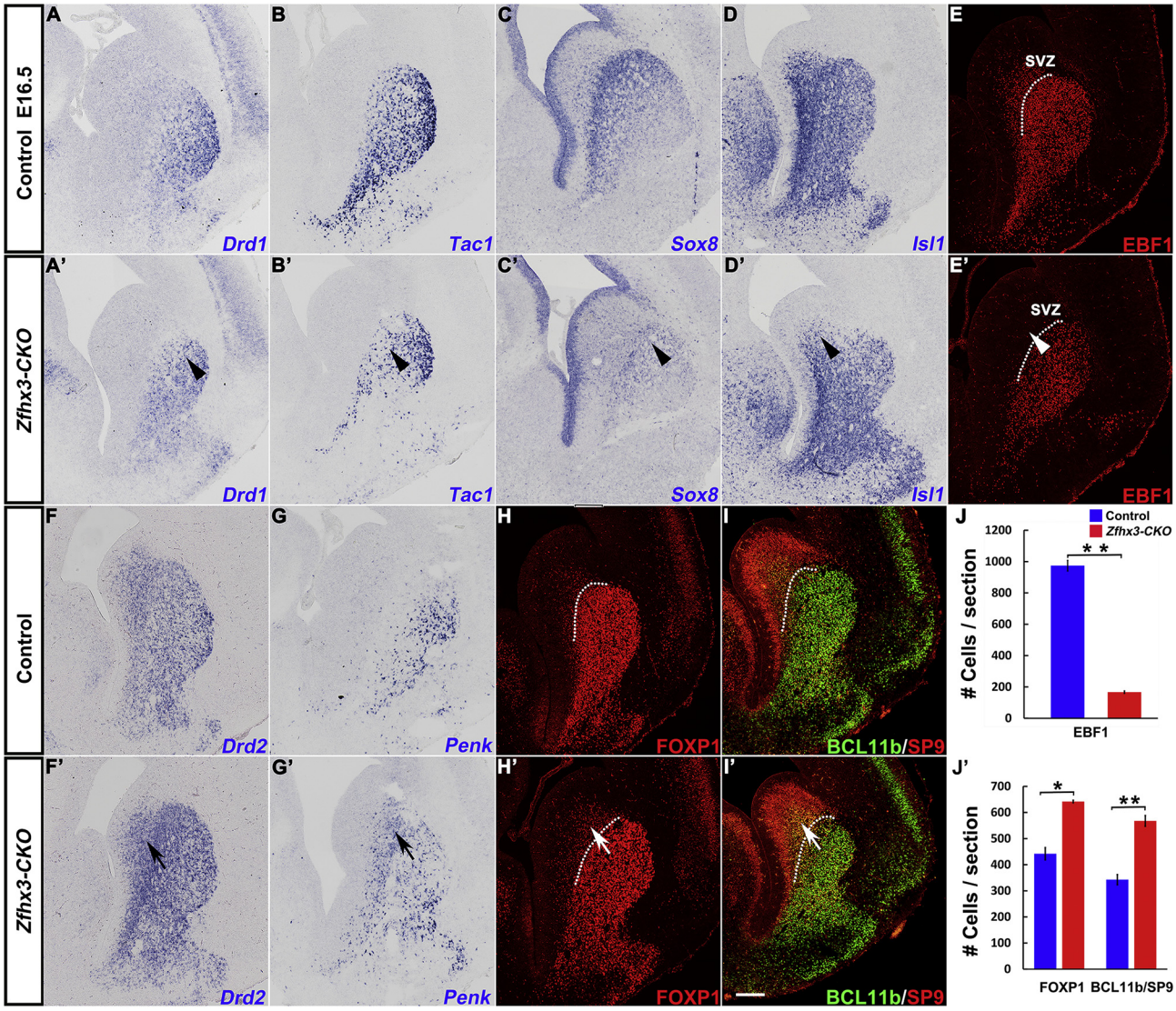


**Fig. 6.** *Zfhx3* promotes D1 MSN differentiation.
(A-G′) Expression of *Drd1, Tac1, Sox8, Isl1* and EBF1 in the LGE was decreased (arrowheads), but *Drd2* and *Penk* expression was increased (arrows) in *Zfhx3-CKO* mice compared to controls at E16.5. (H-I′) More FOXP1$^+$ and BCL11b$^+$/SP9$^+$ cells were observed in the LGE SVZ of *Zfhx3-CKO* mice (arrows). (J, J′) Quantification of above experiments. Dotted lines mark the border of the LGE SVZ and MZ. (Student's *t*-test, *P < .05, **P < .01, n = 3 mice per group, mean ± SEM). Scale bar: 400 μm in I′ for A-I′.

We next examined the MSN projections. Dopamine- and cAMP-regulated neuronal phosphoprotein 32 (DARPP-32, also known as *Ppp1r1b*) is a phosphoprotein that marks all striatal-projection neurons with the exclusion of interneuron populations (Anderson and Reiner, 1991). We stained DARPP-32 at P11 of *Zfhx3-CKO* mouse brains. Despite apparently normal projections to the globus pallidus in the *Zfhx3-CKO* mice, the DARPP-32 staining along the direct pathway tract and in the SNr was reduced (Fig. 5A, B). To further confirm the alterations of the direct pathway, we examined the expression of *Dlx5/6-GFP* at P11, and found that GFP expression pattern was very similar to DARPP-32 (Fig. 5C, D), further suggesting that *Zfhx3* is required for the development of the D1 MSNs.

### 3.4. RNA-Seq analysis reveals molecular defects in the Zfhx3-CKO LGE at E16.5

To further detect the molecular changes in the LGE of *Zfhx3-CKO* mice, we performed RNA-Seq analysis at E16.5 and compared them to their littermate controls. The gene expression levels were reported in FPKM (fragments per kb per million reads) (Trapnell et al., 2012). Our RNA-Seq analysis revealed that about 3700 genes changed their expression levels in the *Zfhx3-CKO* mice (1620 downregulated and 2108 upregulated RNA expression), indicating that *Zfhx3* played a key role in the development of the LGE. Initially, we analyzed the genes which were downregulated in *Zfhx3-CKO* mice. The data showed that the striatal pan-neuronal markers: *Rarb, Foxp1, Zfp503, Plk2* and *Foxp4* and the gene preferences for the D1 MSNs: *Ebf1, Sox8, Foxo1, Isl1, Cdh8, Nrxn1, Slc35d3, Stmn2, Zfp521* and *Chrm4* (Fig. 7H) were grossly reduced. Next, compared to controls, we found that the expression of D2 MSN markers *Penk, Adora2a, Sp9, Drd2* and *Six3* were increased (Fig. 7H). Additionally, the mRNA levels of LGE progenitor-enriched genes were increased, as observed in *Gsx2, Dlx2, Ascl1, Dll3, Hes1, Gadd45g, E2f1, Foxg1* and *Sox4* (Fig. 7H). Thus, these data suggest that *Zfhx3* might have a dual role in promoting D1 and repressing D2 MSN genetic programs.

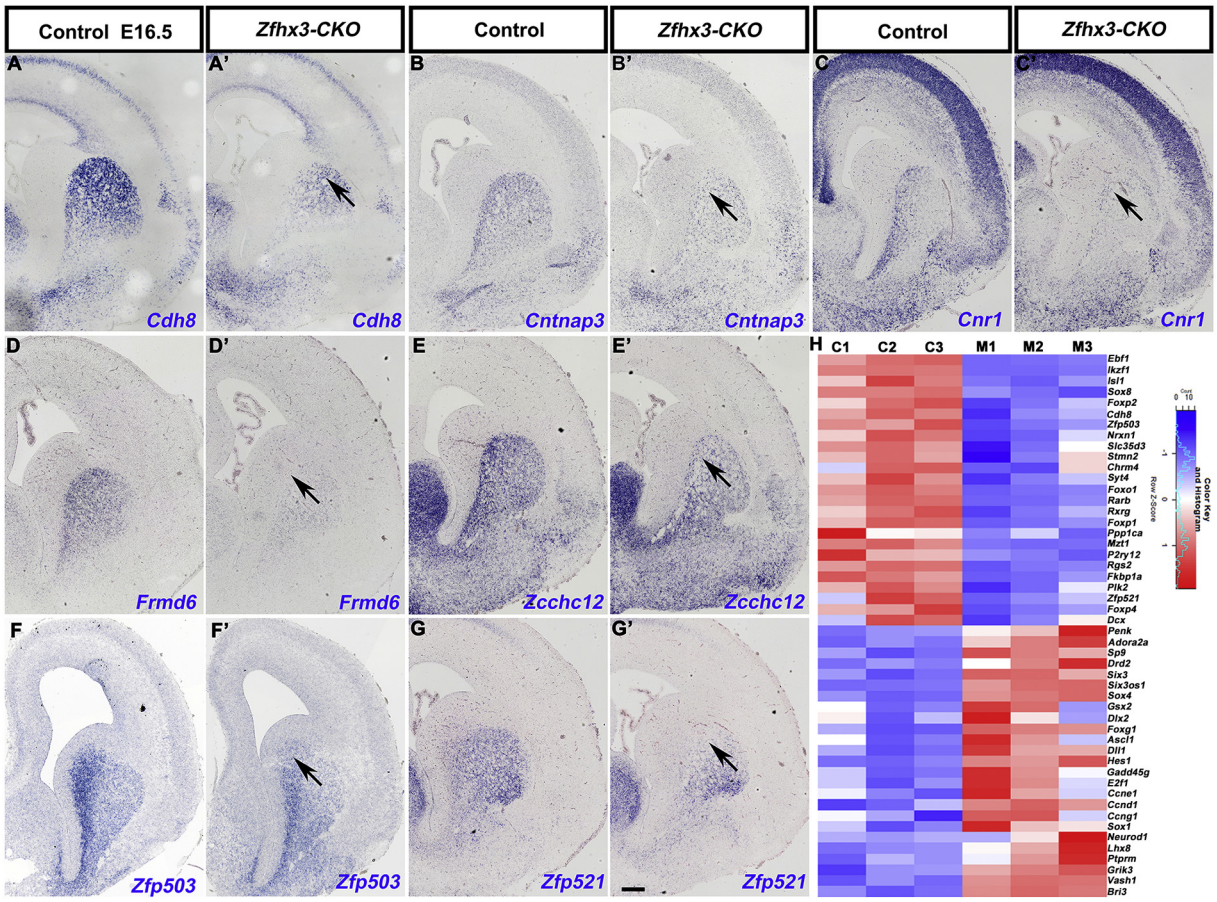


**Fig. 7.** *Zfhx3* promotes the expression of the D1 MSN-enriched genes.
(A-G′) *In situ* RNA hybridization showed that expression of *Cdh8*, *Cntnap3*, *Cnr1*, *Frmd6*, *Zcchc12*, *Zfp503* and *Zfp521* in the LGE was reduced in *Zfhx3-CKO* mice at E16.5 (arrows). (H) Heatmap of selected gene expression in the LGE at E16.5 between control and *Zfhx3-CKO* mice. C1, C2 and C3 represent three biological repeats (control group); M1, M2 and M3 represent the *Zfhx3-CKO* group. n = 3 mice per group, Scale bar: 200 μm in G′ for A-G′.

### 3.5. *Zfhx3 promotes D1 MSN differentiation during development*

To verify the RNA-Seq data, we examined the expression levels of *Drd1*, *Tac1*, *Sox8*, *Drd2* and *Penk* in the LGE at E16.5 (Gerfen et al., 1990; Merchan-Sala et al., 2017). In *Zfhx3-CKO* mice, the expression of *Drd1*, *Tac1, Sox8* and *Isl1* was reduced (Fig. 6A-D′). However, the expression of *Drd2* and *Penk* was increased in the LGE, especially in the SVZ and SVZ/MZ boundary, as shown by *in situ* hybridization (Fig. 6F-G′). We also performed EBF1, FOXP1 and BCL11b/SP9 immunostaining. EBF1 represents a differentiating marker of D1 MSNs and FOXP1$^+$ and BCL11b$^+$/SP9$^+$ cells can be considered D2 MSNs in the LGE SVZ (Arlotta et al., 2008; Gokce et al., 2016; Tamura et al., 2004; Xu et al., 2018; Zhang et al., 2016). We found EBF1$^+$ cells dramatically decreased in the striatal SVZ of *Zfhx3-CKO* mice (Fig. 6E, E′, J). Nevertheless, we observed a 40% increase in the striatal SVZ marked by FOXP1 staining in *Zfhx3-CKO* mice (Fig. 6H, H′, J′). Remarkably, the BCL11b$^+$/SP9$^+$ cells were increased by about 60% in the *Zfhx3-CKO* LGE SVZ compared to the controls (Fig. 6I, I′, J′).

To further address the role of *Zfhx3* in the development of D1 MSNs, we performed *in situ* hybridization for 7 selected genes. These genes were expressed in different developmental steps of the striatal projection neurons. Initially, we analyzed the genes that were expressed in a subpopulation of MSNs which included *Cdh8, Cntnap3* and *Cnr1* (Hirata et al., 2016; Ho et al., 2018; Korematsu and Redies, 1997; Memi et al., 2018; Ruiz-Calvo et al., 2018). Our results showed that these genes were grossly reduced in the *Zfhx3-CKO* mouse striatum (Fig. 7A-C′). Next, we tested the genes that were involved in cell migration and invasion, *Frmd6* and *Zcchc12* (Wang et al., 2017; Xu et al., 2016). In the *Zfhx3-CKO* mice, the expression of *Frmd6* and *Zcchc12* was downregulated, especially for *Frmd6* (Fig. 7D-E′). Finally, we detected the expression of genes related to MSN differentiation, *Zfp503* and *Zfp521* (Chang et al., 2004; Chang et al., 2013; Kamiya et al., 2011; Ko et al., 2013; Shen et al., 2011; Waclaw et al., 2017). The expression of both *Zfp503* and *Zfp521* was noticeably reduced in the *Zfhx3-CKO* striatum (Fig. 7F-G′).

Taken together, these findings suggest that *Zfhx3* promotes the development of striatal D1 MSNs. In the absence of *Zfhx3*, the production of D1 MSNs was compromised whereas, conversely, the differentiation of D2 MSNs was partially increased in the LGE, at least at E16.5.

### 3.6. *Neural progenitors accumulate in the LGE SVZ of Zfhx3-CKO mice at E16.5*

In the *Zfhx3-CKO* mice, we observed more GSX2$^+$ and ASCL1$^+$ cells in the LGE SVZ compared with controls (Fig. 8A-B′), consistent with our RNA-Seq analysis. Quantification data showed that GSX2$^+$ and ASCL1$^+$ cells in the *Zfhx3-CKO* mice LGE SVZ were increased 1.6 and 2.2 times, respectively (Fig. 8C, D). The previous study showed that ASCL1 activated different regulators to promote and terminate the cell cycle (Castro et al., 2011). Indeed, our RNA-Seq data showed that *Ascl1* and its target genes *E2f1* and *Hes1*, which promote cell cycle and maintenance of the progenitor state, and *Gadd45g*, which inhibits cell cycle in the Zfhx*3-CKO* mice were upregulated (Fig. 7H). Thus, these results suggested that without *Zfhx3* function, the differentiation of LGE SVZ progenitors was blocked, leading to an accumulation of neural progenitors in the LGE SVZ.

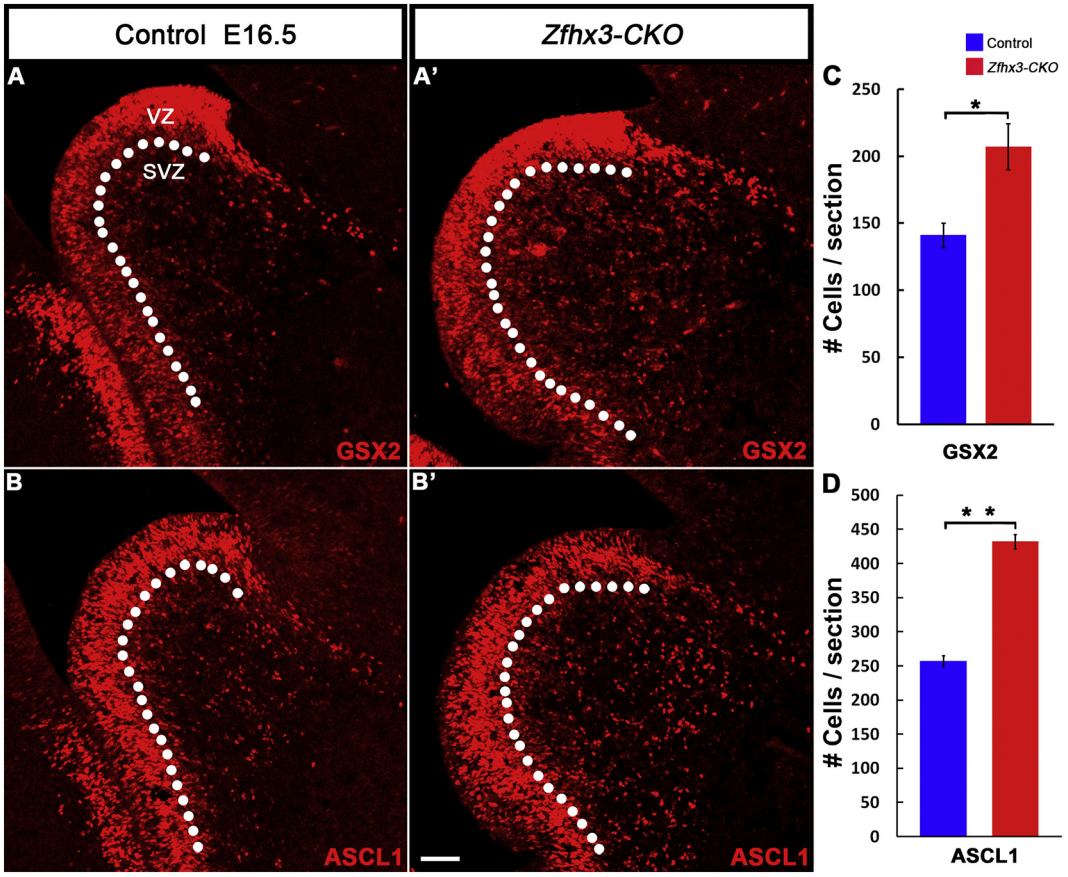


**Fig. 8.** Neural progenitor cells accumulate in the LGE SVZ of *Zfhx3-CKO* mice at E16.5.
(A-D) *Zfhx3-CKO* mice had more GSX2$^+$ and ASCL1$^+$ neural progenitors in the LGE SVZ than controls (Student's *t*-test, *P < .05, **P < .01, n = 3 mice per group, mean ± SEM). Dotted lines mark the LGE VZ/SVZ boundary. 200 μm in B′ for A-B′.

### 3.7. Zfhx3 is critical for the differentiation of late born D1 MSNs

As described above, the D1 MSNs were selectively reduced in the *Zfhx3-CKO* striatum at P11 (Fig. 4A-B′). We hypothesized that *Zfhx3* affects the differentiation of immature neurons and leads to cell death. To test this idea, we analyzed the expression of the MSN marker FOXP1 and the D1 MSN markers EBF1 and ISL1 at P0. Consistent with the above results, there was a reduction in the FOXP1$^+$ cells (Fig. 9A, A′, data not shown). Remarkably, the expression of EBF1 and *Isl1* mRNA showed a dramatic decrease (Fig. 9B-C′). Previous studies showed that *Dlx1/2* were involved in the neurogenesis of late born striatal MSNs (Anderson et al., 1997; Yun et al., 2002). We examined the expression of *Dlx1* and *Dlx2* in the *Zfhx3-CKO* striatum at P0, and observed that many *Dlx1*$^+$ and DLX2$^+$ cells accumulated in the striatal SVZ of the *Zfhx3-CKO* mice at P0 (Fig. 9D-E′). Enlargement of the SVZ in the *Zfhx3-CKO* mice could be a consequence of the incapacity of progenitor/immature cells to differentiate into striatal MSNs. For this reason, we analyzed MSN neurogenesis at different stages during development. Initially, we injected BrdU at E13.5 and analyzed at E16.5. There were no significant differences in the number of BrdU$^+$ cells in the striatum (LGE MZ) of the controls compared to the *Zfhx3-CKO* mice (Fig. 9G-G′, H). However, there were significantly decreased BrdU$^+$ cells in the striatum of the *Zfhx3-CKO* mice compared to controls when BrdU was injected at E16.5 and analyzed at P0 (Fig. 9F-F′, H). Moreover, many BrdU$^+$ cells accumulated in the striatal SVZ of the *Zfhx3-CKO* mice (Fig. 9F-F′), further indicating the differentiation defects of late born D1 MSNs.

### 3.8. Increased apoptosis in the postnatal striatum of Zfhx3-CKO mice

To examine apoptotic cell death in the LGE and striatum, immunostaining with Cleaved Caspase-3 was performed and did not reveal any differences between the *Zfhx3-CKO* and control mice at E14.5 and E17.5 (data not shown). However, a significant increase in the number of apoptotic cells was detected in the SVZ and medial part of the striatum at P3 in *Zfhx3-CKO* mice (Fig. 10C, D, C′ and D′). This cell death continues to P7 and normalizes at P11 (Fig. 10A-J, K). Therefore, loss of *Zfhx3* might produce a dysfunction in the time and position of late born D1 MSNs in the striatum. These effects had also been previously described in *Isl1* and *Ebf1* mutant mice (Ehrman et al., 2013; Garel et al., 1999; Lobo et al., 2008; Lu et al., 2014). In conclusion, our results suggest that the cell death observed in the *Zfhx3-CKO* mice could be a consequence of blocked differentiation of late born D1 MSNs.

## 4. Discussion

In the present study, we show that *Zfhx3* is selectively expressed in post-mitotic immature striatal D1 MSNs. Loss of *Zfhx3* function results in reduced numbers of D1 MSNs, whereas D2 MSNs remained largely unaffected. We propose three main reasons to explain this phenotype: 1) The differentiation of LGE neural progenitors was blocked, resulting in more progenitors accumulating in the LGE SVZ; 2) Late born D1 MSNs failed to differentiate; and 3) Apoptotic cell death occurred in the postnatal striatum during the first week. Many diseases, such as Huntington's disease (HD) and attention deficit/hyperactivity disorder (ADHD), are associated with loss of striatal MSNs (Albin et al., 1989; Gerfen and Surmeier, 2011; Leisman and Melillo, 2013). Moreover, aberrant basal ganglion circuitry leads to locomotor dysfunction. Thus,

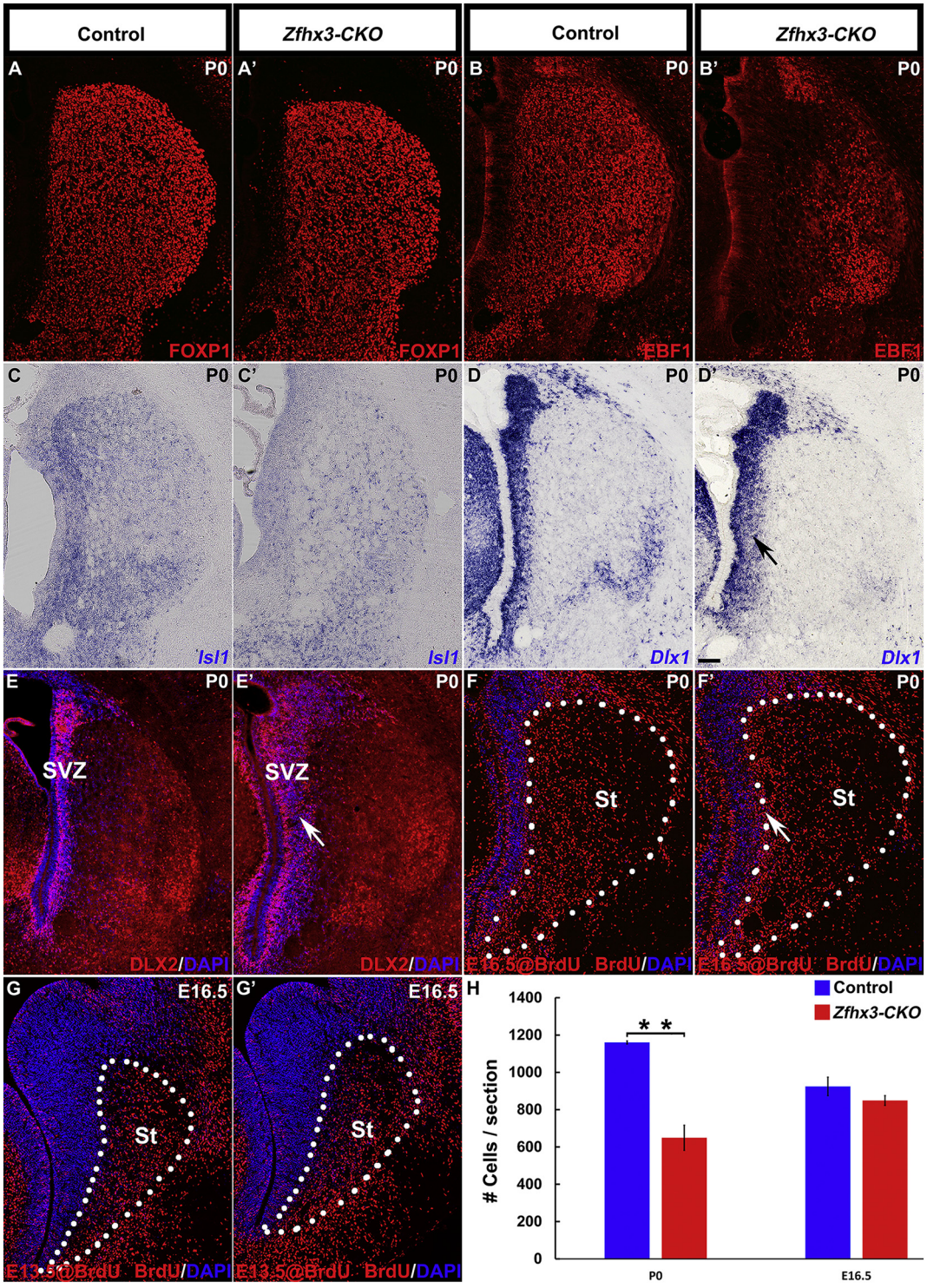


**Fig. 9.** The late born D1 MSNs are reduced in the striatum of *Zfhx3-CKO* mice.
(A-C′) There was a slight reduction in the expression of FOXP1 whereas, there was a severe reduction in EBF1 and *Isl1* in the mutant striatum at P0. (D-E′) Many *Dlx1*$^+$ and DLX2$^+$ cells accumulated in the *Zfhx3-CKO* mouse SVZ compared to controls (arrows). (F-F′) BrdU was injected intraperitoneally at E16.5 and then mice were sacrificed at P0. Immunostaining of BrdU showed that the *Zfhx3-CKO* mice had fewer BrdU$^+$ cells in the striatum relative to controls. Note that many BrdU$^+$ cells accumulated in the *Zfhx3-CKO* mice striatal SVZ (arrow). (G, G′, H) BrdU was injected intraperitoneally at E13.5 and then mice were sacrificed at E16.5. The number of BrdU$^+$ cells in the *Zfhx3-CKO* striatum was comparable to controls. (Student's *t*-test, **P < .01, n = 3 mice per group, mean ± SEM). Dotted lines mark the border of the striatum. Scale bars: 200 μm in D′ for A-G′.

our *Zfhx3-CKO* mice might serve as a model to study D1 MSN function in the striatum and basal ganglion disorders caused by loss of D1 MSNs.

### 4.1. *Zfhx3 is selectively expressed in post-mitotic immature striatal D1 MSNs during LGE development*

Normal development of striatal MSNs requires multiple

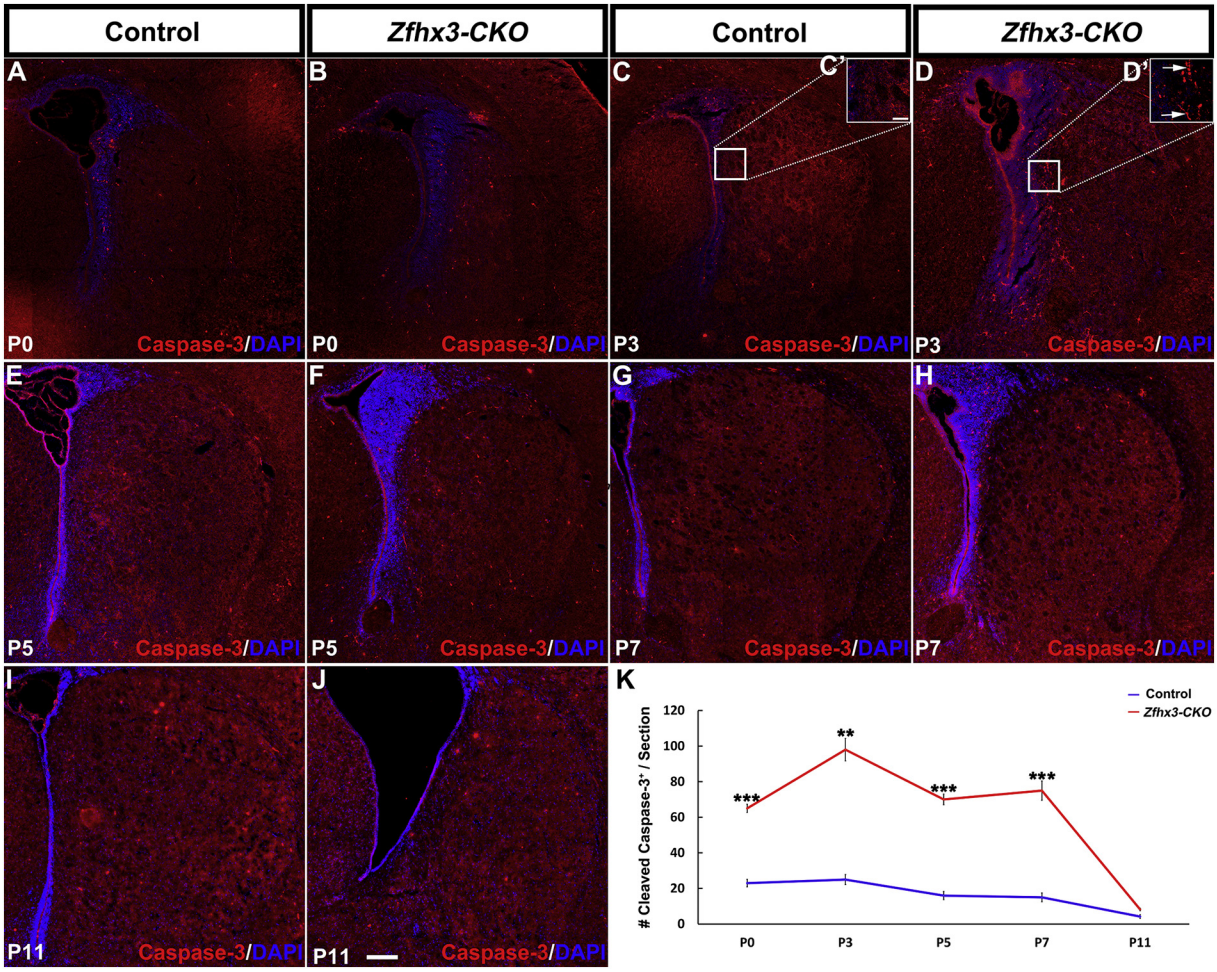


**Fig. 10.** Loss of *Zfhx3* results in increased apoptosis in the postnatal striatum.
(A-J) Immunostaining images showed that compared to controls there were more Cleaved Caspase-3$^+$ cells in the SVZ and medial part of the striatum in *Zfhx3-CKO* mice at different stages (P0, P3, P5 and P7). Note the smaller striatum and larger lateral ventricle in *Zfhx3-CKO* mice. (C′, D′) Higher magnification images of the boxed area in (C, D). Arrows indicate the Cleaved Caspase-3$^+$ cells. (K) Quantification of the number of Cleaved Caspase-3$^+$ cells showed that apoptosis mainly occurs from P0 to P7. (One-way ANOVA followed by Tukey-Kramer *post hoc* test, **P $<$ .01, ***P $<$ .001, n = 3 mice per group, mean $\pm$ SEM). Scale bars: 200 μm in J for A-J; 50 μm in C′ for C′ and D′.

transcription factors to correctly switch on/off at the appropriate times. These transcriptional factors can be divided into two groups, which are involved in the development of the striatum. One group is robustly expressed at embryonic developmental stages, downregulates after birth. These genes mainly include *Ebf1*, *Isl1*, *Ikaros-1 (Ikzf1)*, *Helios (Ikzf2)* and *Zfp503* known for their involvement in the production, differentiation and migration of striatal projection neurons (Chang et al., 2013; Ehrman et al., 2013; Garel et al., 1999; Ko et al., 2013; Lobo et al., 2006; Lobo et al., 2008; Martin-Ibanez et al., 2012; Martin-Ibanez et al., 2010; Martin-Ibanez et al., 2017; Novak et al., 2013). The other group, initially expressed during the embryonic stage, is maintained throughout adulthood and mainly includes *Sp9, Bcl11b, Sox8, Foxp1* and *Foxo1* playing roles in differentiation, maturation and survival of striatal MSNs (Arlotta et al., 2008; Bacon et al., 2015; Baydyuk et al., 2011; Leid et al., 2004; Li et al., 2012; Tamura et al., 2004; Waclaw et al., 2017; Zhang et al., 2016). We found that *Zfhx3* is a developmentally regulated striatum-enriched gene. *Zfhx3* is strongly expressed in the LGE SVZ/MZ boundary, but its expression in the striatum is dramatically downregulated in the first postnatal week. Because *Zfhx3* is selectively expressed in post-mitotic immature striatal D1 MSNs during development, it can be used as a novel marker for studies associated with D1 MSNs.

### 4.2. Loss of Zfhx3 function disrupts D1 MSN progenitor differentiation

In *Zfhx3-CKO* mutants, neural progenitors accumulate in the SVZ. These cells have increased GSX2 and ASCL1 transcription factor expression, providing strong evidence that they are arrested as immature neural progenitors (Li et al., 2017; Xu et al., 2018). Furthermore, since ASCL1 directly drives *Dll1* (delta-like 1) expression, it increases Notch signaling in adjacent cells and thereby, promotes the maintenance of their progenitor state (Casarosa et al., 1999; Castro et al., 2011). In addition, recent studies showed that ASCL1 promoted expression of genes that inhibited cell cycle progression and/or promoted cell cycle arrest (Casarosa et al., 1999; Castro et al., 2011). Using BrdU birth-dating analysis, we observed that the production of late born MSNs was compromised, whereas early born MSNs were largely unaffected. This was consistent with observations that there were more progenitors in the LGE SVZ at E16.5 as well as in striatal SVZ at P0, but EBF1$^+$ and ISL1$^+$ D1 MSNs were severely reduced in the striatum.

### 4.3. Zfhx3 has a minor role in D2 MSN development

In the striatum, we observed that the numbers of D2 MSNs were similar between control and *Zfhx3-CKO* mice. In the E16.5 LGE SVZ, however, there were more D2 MSNs in *Zfhx3-CKO* mice compared to

controls, including *Drd2*$^{+}$, *Penk*$^{+}$, FOXP1$^{+}$ and Bcl11b$^{+}$/SP9$^{+}$ cells (Fig. 6F-I′, J′). *Foxp1* in the LGE SVZ is preferentially expressed in immature D2 MSNs (Gokce et al., 2016). Thus, an increase in post-mitotic young D2 MSNs in the LGE SVZ provides evidence that their development may be abnormal. This could be, however, a compensation for the reduction of D1 MSN production. We propose that the temporary increase in D2 MSN production in the E16.5 LGE SVZ of *Zfhx3-CKO* mice does not directly demonstrate their abnormal development.

### 4.4. Apoptotic cell death in the postnatal striatum of Zfhx3-CKO mice

In the LGE SVZ and P0 striatal SVZ of the *Zfhx3-CKO* mice, there was more neural progenitor accumulation. This resulted from the differentiation defects of late born MSNs. Accordingly, in *Zfhx3-CKO* mice the loss of D1 MSNs was mainly observed in the medial part of the striatum. Interestingly, apoptosis was also prevalent in this region in the early postnatal period. We propose that these undifferentiated MSNs especially the immature D1 MSNs, undergo apoptotic cell death, finally resulting in about a 30% loss in the P11 striatum.

## Author contributions

Z.Z. and S.W. performed experiments and analysis. H.D, S.Z., Y.W., G.T., Z.S., X.S., Z.X., and Y.Y. helped conduct experiments. Z.Y. and Z.Z. designed the experiments and analyzed the results and wrote the paper.

## Funding

Research grants to Z.Yang. from National Key Research and Development Program of China (2018YFA0108000), National Natural Science Foundation of China (NSFC 31820103006, 31630032, 31425011, and 31429002), research grant to Y. You (NSFC 31700889).

## Declaration of Competing Interest

None of the author has any conflict of interest to declare.

## Acknowledgements

We are grateful to Jintang Dong at Emory University for the generous gift of *Zfhx3*$^{F/+}$ mice, and Kenneth Campbell at University of Cincinnati College of Medicine for *Dlx5/6-Cre* mice. The authors thank Kazuaki Yoshikawa for providing the DLX2 antibody.

## References

Albin, R.L., Young, A.B., Penney, J.B., 1989. The functional anatomy of basal ganglia disorders. Trends Neurosci. 366–375. https://doi.org/10.1016/0166-2236(89)90074-X.

Anderson, K.D., Reiner, A., 1991. Immunohistochemical localization of DARPP-32 in striatal projection neurons and striatal interneurons: implications for the localization of D1-like dopamine receptors on different types of striatal neurons. Brain Res. 568, 235–243. https://doi.org/10.1016/0006-8993(91)91403-N.

Anderson, S.A., Qiu, M., Bulfone, A., Eisenstat, D.D., Meneses, J., Pedersen, R., Rubenstein, J.L., 1997. Mutations of the homeobox genes Dlx-1 and Dlx-2 disrupt the striatal subventricular zone and differentiation of late born striatal neurons. Neuron 19, 27–37. https://doi.org/10.1016/S0896-6273(00)80345-1.

Arlotta, P., Molyneaux, B.J., Jabaudon, D., Yoshida, Y., Macklis, J.D., 2008. Ctip2 controls the differentiation of medium spiny neurons and the establishment of the cellular architecture of the striatum. J. Neurosci. 28, 622–632. https://doi.org/10.1523/JNEUROSCI.2986-07.2008.

Bacon, C., Schneider, M., Le Magueresse, C., Froehlich, H., Sticht, C., Gluch, C., Monyer, H., Rappold, G.A., 2015. Brain-specific Foxp1 deletion impairs neuronal development and causes autistic-like behaviour. Mol. Psychiatry 20, 632–639. https://doi.org/10.1038/mp.2014.116.

Baydyuk, M., Russell, T., Liao, G.Y., Zang, K., An, J.J., Reichardt, L.F., Xu, B., 2011. TrkB receptor controls striatal formation by regulating the number of newborn striatal neurons. Proc. Natl. Acad. Sci. U. S. A. 108, 1669–1674. https://doi.org/10.1073/pnas.1004744108.

Bertran-Gonzalez, J., Bosch, C., Maroteaux, M., Matamales, M., Herve, D., Valjent, E., Girault, J.A., 2008. Opposing patterns of signaling activation in dopamine D1 and D2 receptor-expressing striatal neurons in response to cocaine and haloperidol. J. Neurosci. 28, 5671–5685. https://doi.org/10.1523/JNEUROSCI.1039-08.2008.

Casarosa, S., Fode, C., Guillemot, F., 1999. Mash1 regulates neurogenesis in the ventral telencephalon. Development 525–534.

Castro, D.S., Martynoga, B., Parras, C., Ramesh, V., Pacary, E., Johnston, C., Drechsel, D., Lebel-Potter, M., Garcia, L.G., Hunt, C., Dolle, D., Bithell, A., Ettwiller, L., Buckley, N., Guillemot, F., 2011. A novel function of the proneural factor Ascl1 in progenitor proliferation identified by genome-wide characterization of its targets. Genes Dev. 25, 930–945. https://doi.org/10.1101/gad.627811.

Chang, C.W., Tsai, C.W., Wang, H.F., Tsai, H.C., Chen, H.Y., Tsai, T.F., Takahashi, H., Li, H.Y., Fann, M.J., Yang, C.W., Hayashizaki, Y., Saito, T., Liu, F.C., 2004. Identification of a developmentally regulated striatum-enriched zinc-finger gene, Nolz-1, in the mammalian brain. Proc. Natl. Acad. Sci. U. S. A. 101, 2613–2618. https://doi.org/10.1073/pnas.0308645100.

Chang, S.L., Chen, S.Y., Huang, H.H., Ko, H.A., Liu, P.T., Liu, Y.C., Chen, P.H., Liu, F.C., 2013. Ectopic expression of nolz-1 in neural progenitors promotes cell cycle exit/premature neuronal differentiation accompanying with abnormal apoptosis in the developing mouse telencephalon. PLoS One 8, e74975. https://doi.org/10.1371/journal.pone.0074975.

Chen, Y.J., Friedman, B.A., Ha, C., Durinck, S., Liu, J., Rubenstein, J.L., Seshagiri, S., Modrusan, Z., 2017. Single-cell RNA sequencing identifies distinct mouse medial ganglionic eminence cell types. Sci. Rep. 7, 45656. https://doi.org/10.1038/srep45656.

Cobos, I., Borello, U., Rubenstein, J.L., 2007. Dlx transcription factors promote migration through repression of axon and dendrite growth. Neuron 54, 873–888. https://doi.org/10.1016/j.neuron.2007.05.024.

DeLong, M.R., 1990. Primate models of movement disorders of basal ganglia origin. Trends Neurosci. 13, 281–285. https://doi.org/10.1016/0166-2236(90)90110-V.

Ehrman, L.A., Mu, X., Waclaw, R.R., Yoshida, Y., Vorhees, C.V., Klein, W.H., Campbell, K., 2013. The LIM homeobox gene Isl1 is required for the correct development of the striatonigral pathway in the mouse. Proc. Natl. Acad. Sci. U. S. A. 110, E4026–E4035. https://doi.org/10.1073/pnas.1308275110.

Garel, S., Marin, F., Grosschedl, R., Charnay, P., 1999. Ebf1 controls early cell differentiation in the embryonic striatum. Development 126, 5285–5294.

Gerfen, C.R., 1992. The neostriatal mosaic: multiple levels of compartmental organization. Trends Neurosci. 15, 133–139. https://doi.org/10.1016/0166-2236(92)90355-C.

Gerfen, C.R., Surmeier, D.J., 2011. Modulation of striatal projection systems by dopamine. Annu. Rev. Neurosci. 34, 441–466. https://doi.org/10.1146/annurev-neuro-061010-113641.

Gerfen, C.R., Engber, T.M., Mahan, L.C., Susel, Z., Chase, T.N., Monsma Jr., F.J., Sibley, D.R., 1990. D1 and D2 dopamine receptor-regulated gene expression of striatonigral and striatopallidal neurons. Science 250, 1429–1432. https://doi.org/10.1126/science.2147780.

Gokce, O., Stanley, G.M., Treutlein, B., Neff, N.F., Camp, J.G., Malenka, R.C., Rothwell, P.E., Fuccillo, M.V., Sudhof, T.C., Quake, S.R., 2016. Cellular taxonomy of the mouse striatum as revealed by single-cell RNA-Seq. Cell Rep. 16, 1126–1137. https://doi.org/10.1016/j.celrep.2016.06.059.

Gong, S., Doughty, M., Harbaugh, C.R., Cummins, A., Hatten, M.E., Heintz, N., Gerfen, C.R., 2007. Targeting Cre recombinase to specific neuron populations with bacterial artificial chromosome constructs. J. Neurosci. 27, 9817–9823. https://doi.org/10.1523/JNEUROSCI.2707-07.2007.

Hansen, D.V., Lui, J.H., Flandin, P., Yoshikawa, K., Rubenstein, J.L., Alvarez-Buylla, A., Kriegstein, A.R., 2013. Non-epithelial stem cells and cortical interneuron production in the human ganglionic eminences. Nat. Neurosci. 16, 1576–1587. https://doi.org/10.1038/nn.3541.

Hirata, H., Umemori, J., Yoshioka, H., Koide, T., Watanabe, K., Shimoda, Y., 2016. Cell adhesion molecule contactin-associated protein 3 is expressed in the mouse basal ganglia during early postnatal stages. J. Neurosci. Res. 94, 74–89. https://doi.org/10.1002/jnr.23670.

Ho, H., Both, M., Siniard, A., Sharma, S., Notwell, J.H., Wallace, M., Leone, D.P., Nguyen, A., Zhao, E., Lee, H., Zwilling, D., Thompson, K.R., Braithwaite, S.P., Huentelman, M., Portmann, T., 2018. A guide to single-cell transcriptomics in adult rodent brain: the medium spiny neuron transcriptome revisited. Front. Cell. Neurosci. 12, 159. https://doi.org/10.3389/fncel.2018.00159.

Jung, C.G., Kim, H.J., Kawaguchi, M., Khanna, K.K., Hida, H., Asai, K., Nishino, H., Miura, Y., 2005. Homeotic factor ATBF1 induces the cell cycle arrest associated with neuronal differentiation. Development 132, 5137–5145. https://doi.org/10.1242/dev.02098.

Kamiya, D., Banno, S., Sasai, N., Ohgushi, M., Inomata, H., Watanabe, K., Kawada, M., Yakura, R., Kiyonari, H., Nakao, K., Jakt, L.M., Nishikawa, S., Sasai, Y., 2011. Intrinsic transition of embryonic stem-cell differentiation into neural progenitors. Nature 470, 503–509. https://doi.org/10.1038/nature09726.

Ko, H.A., Chen, S.Y., Chen, H.Y., Hao, H.J., Liu, F.C., 2013. Cell type-selective expression of the zinc finger-containing gene Nolz-1/Zfp503 in the developing mouse striatum. Neurosci. Lett. 548, 44–49. https://doi.org/10.1016/j.neulet.2013.05.020.

Korematsu, K., Redies, C., 1997. Expression of cadherin-8 mRNA in the developing mouse central nervous system. J. Comp. Neurol. 387, 291–306. https://doi.org/10.1002/(SICI)1096-9861(19971020)387:2%3C291::AID-CNE10%3E3.0.CO;2-Y.

Kuwajima, T., Nishimura, I., Yoshikawa, K., 2006. Necdin promotes GABAergic neuron differentiation in cooperation with Dlx homeodomain proteins. J. Neurosci. 26, 5383–5392. https://doi.org/10.1523/JNEUROSCI.1262-06.2006.

Leid, M., Ishmael, J.E., Avram, D., Shepherd, D., Fraulob, V., Dolle, P., 2004. CTIP1 and CTIP2 are differentially expressed during mouse embryogenesis. Gene Expr. Patterns 4, 733–739. https://doi.org/10.1016/j.modgep.2004.03.009.

Leisman, G., Melillo, R., 2013. The basal ganglia: motor and cognitive relationships in a

clinical neurobehavioral context. Rev. Neurosci. 24, 9–25. https://doi.org/10.1515/revneuro-2012-0067.
Li, Y., Yui, D., Luikart, B.W., McKay, R.M., Li, Y., Rubenstein, J.L., Parada, L.F., 2012. Conditional ablation of brain-derived neurotrophic factor-TrkB signaling impairs striatal neuron development. Proc. Natl. Acad. Sci. U. S. A. 109, 15491–15496. https://doi.org/10.1073/pnas.1212899109.
Li, J., Wang, C., Zhang, Z., Wen, Y., An, L., Liang, Q., Xu, Z., Wei, S., Li, W., Guo, T., Liu, G., Tao, G., You, Y., Du, H., Fu, Z., He, M., Chen, B., Campbell, K., Alvarez-Buylla, A., Rubenstein, J.L., Yang, Z., 2017. Transcription factors Sp8 and Sp9 coordinately regulate olfactory bulb interneuron development. Cereb. Cortex 1–17. https://doi.org/10.1093/cercor/bhx199.
Liu, F., You, Y., Li, X., Ma, T., Nie, Y., Wei, B., Li, T., Lin, H., Yang, Z., 2009. Brain injury does not alter the intrinsic differentiation potential of adult neuroblasts. J. Neurosci. 29, 5075–5087. https://doi.org/10.1523/JNEUROSCI.0201-09.2009.
Lobo, M.K., Karsten, S.L., Gray, M., Geschwind, D.H., Yang, X.W., 2006. FACS-array profiling of striatal projection neuron subtypes in juvenile and adult mouse brains. Nat. Neurosci. 9, 443–452. https://doi.org/10.1038/nn1654.
Lobo, M.K., Yeh, C., Yang, X.W., 2008. Pivotal role of early B-cell factor 1 in development of striatonigral medium spiny neurons in the matrix compartment. J. Neurosci. Res. 86, 2134–2146. https://doi.org/10.1002/jnr.21666.
Lu, K.M., Evans, S.M., Hirano, S., Liu, F.C., 2014. Dual role for Islet-1 in promoting striatonigral and repressing striatopallidal genetic programs to specify striatonigral cell identity. Proc. Natl. Acad. Sci. U. S. A. 111, E168–E177. https://doi.org/10.1073/pnas.1319138111.
Lundell, M.J., Hirsh, J., 1992. The zfh-2 gene product is a potential regulator of neuron-specific dopa decarboxylase gene expression in Drosophila. Dev. Biol. 154, 84–94. https://doi.org/10.1016/0012-1606(92)90050-Q.
Martin-Ibanez, R., Crespo, E., Urban, N., Sergent-Tanguy, S., Herranz, C., Jaumot, M., Valiente, M., Long, J.E., Pineda, J.R., Andreu, C., Rubenstein, J.L., Marin, O., Georgopoulos, K., Mengod, G., Farinas, I., Bachs, O., Alberch, J., Canals, J.M., 2010. Ikaros-1 couples cell cycle arrest of late striatal precursors with neurogenesis of enkephalinergic neurons. J. Comp. Neurol. 518, 329–351. https://doi.org/10.1002/cne.22215.
Martin-Ibanez, R., Crespo, E., Esgleas, M., Urban, N., Wang, B., Waclaw, R., Georgopoulos, K., Martinez, S., Campbell, K., Vicario-Abejon, C., Alberch, J., Chan, S., Kastner, P., Rubenstein, J.L., Canals, J.M., 2012. Helios transcription factor expression depends on Gsx2 and Dlx1&2 function in developing striatal matrix neurons. Stem Cells Dev. 21, 2239–2251. https://doi.org/10.1089/scd.2011.0607.
Martin-Ibanez, R., Pardo, M., Giralt, A., Miguez, A., Guardia, I., Marion-Poll, L., Herranz, C., Esgleas, M., Garcia-Diaz Barriga, G., Edel, M.J., Vicario-Abejon, C., Alberch, J., Girault, J.A., Chan, S., Kastner, P., Canals, J.M., 2017. Helios expression coordinates the development of a subset of striatopallidal medium spiny neurons. Development 144, 1566–1577. https://doi.org/10.1242/dev.138248.
Mayer, C., Hafemeister, C., Bandler, R.C., Machold, R., Batista Brito, R., Jaglin, X., Allaway, K., Butler, A., Fishell, G., Satija, R., 2018. Developmental diversification of cortical inhibitory interneurons. Nature 555, 457–462. https://doi.org/10.1038/nature25999.
Memi, F., Killen, A.C., Barber, M., Parnavelas, J.G., Andrews, W.D., 2018. Cadherin 8 regulates proliferation of cortical interneuron progenitors. Brain Struct. Funct. https://doi.org/10.1007/s00429-018-1772-4.
Merchan-Sala, P., Nardini, D., Waclaw, R.R., Campbell, K., 2017. Selective neuronal expression of the SoxE factor, Sox8, in direct pathway striatal projection neurons of the developing mouse brain. J. Comp. Neurol. 525, 2805–2819. https://doi.org/10.1002/cne.24232.
Morinaga, T., Yasuda, H., Hashimoto, T., Higashio, K., Tamaoki, T., 1991. A human alpha-fetoprotein enhancer-binding protein, ATBF1, contains four homeodomains and seventeen zinc fingers. Mol. Cell. Biol. 11, 6041–6049. https://doi.org/10.1128/MCB.11.12.6041.
Novak, G., Fan, T., O'Dowd, B.F., George, S.R., 2013. Striatal development involves a switch in gene expression networks, followed by a myelination event: implications for neuropsychiatric disease. Synapse 67, 179–188. https://doi.org/10.1002/syn.21628.
Olsson, M., Campbell, K., Wictorin, K., Bjorklund, A., 1995. Projection neurons in fetal striatal transplants are predominantly derived from the lateral ganglionic eminence. Neuroscience 69, 1169–1182. https://doi.org/10.1016/0306-4522(95)00325-D.
Oude Ophuis, R.J., Boender, A.J., van Rozen, A.J., Adan, R.A., 2014. Cannabinoid, melanocortin and opioid receptor expression on DRD1 and DRD2 subpopulations in rat striatum. Front. Neuroanat. 8, 14. https://doi.org/10.3389/fnana.2014.00014.
Perreault, M.L., Hasbi, A., Alijaniaram, M., Fan, T., Varghese, G., Fletcher, P.J., Seeman, P., O'Dowd, B.F., George, S.R., 2010. The dopamine D1-D2 receptor heteromer localizes in dynorphin/enkephalin neurons: increased high affinity state following amphetamine and in schizophrenia. J. Biol. Chem. 285, 36625–36634. https://doi.org/10.1074/jbc.M110.159954.
Perreault, M.L., Fan, T., Alijaniaram, M., O'Dowd, B.F., George, S.R., 2012. Dopamine D1-D2 receptor heteromer in dual phenotype GABA/glutamate-coexpressing striatal medium spiny neurons: regulation of BDNF, GAD67 and VGLUT1/2. PLoS One 7, e33348. https://doi.org/10.1371/journal.pone.0033348.
Ruiz-Calvo, A., Maroto, I.B., Bajo-Graneras, R., Chiarlone, A., Gaudioso, A., Ferrero, J.J., Resel, E., Sanchez-Prieto, J., Rodriguez-Navarro, J.A., Marsicano, G., Galve-Roperh, I., Bellocchio, L., Guzman, M., 2018. Pathway-specific control of striatal neuron vulnerability by corticostriatal cannabinoid CB1 receptors. Cereb. Cortex 28, 307–322. https://doi.org/10.1093/cercor/bhx285.
Shen, S., Pu, J., Lang, B., McCaig, C.D., 2011. A zinc finger protein Zfp521 directs neural differentiation and beyond. Stem Cell Res Ther 2, 20. https://doi.org/10.1186/scrt61.
Stenman, J., Toresson, H., Campbell, K., 2003. Identification of two distinct progenitor populations in the lateral ganglionic eminence: implications for striatal and olfactory bulb neurogenesis. J. Neurosci. 23, 167–174. https://doi.org/10.1523/JNEUROSCI.23-01-00167.2003.
Sun, X., Fu, X., Li, J., Xing, C., Martin, D.W., Zhang, H.H., Chen, Z., Dong, J.T., 2012. Heterozygous deletion of Atbf1 by the Cre-loxP system in mice causes preweaning mortality. Genesis 50, 819–827. https://doi.org/10.1002/dvg.22041.
Tamura, S., Morikawa, Y., Iwanishi, H., Hisaoka, T., Senba, E., 2004. Foxp1 gene expression in projection neurons of the mouse striatum. Neuroscience 124, 261–267. https://doi.org/10.1016/j.neuroscience.2003.11.036.
Trapnell, C., Roberts, A., Goff, L., Pertea, G., Kim, D., Kelley, D.R., Pimentel, H., Salzberg, S.L., Rinn, J.L., Pachter, L., 2012. Differential gene and transcript expression analysis of RNA-seq experiments with TopHat and Cufflinks. Nat. Protoc. 7, 562–578. https://doi.org/10.1038/nprot.2012.016.
van Rhijn, J.-R., Fisher, S.E., Vernes, S.C., Nadif Kasri, N., 2018. Foxp2 loss of function increases striatal direct pathway inhibition via increased GABA release. Brain Struct. Funct. https://doi.org/10.1007/s00429-018-1746-6.
Waclaw, R.R., Allen 2nd, Z.J., Bell, S.M., Erdelyi, F., Szabo, G., Potter, S.S., Campbell, K., 2006. The zinc finger transcription factor Sp8 regulates the generation and diversity of olfactory bulb interneurons. Neuron 49, 503–516. https://doi.org/10.1016/j.neuron.2006.01.018.
Waclaw, R.R., Ehrman, L.A., Merchan-Sala, P., Kohli, V., Nardini, D., Campbell, K., 2017. Foxo1 is a downstream effector of Isl1 in direct pathway striatal projection neuron development within the embryonic mouse telencephalon. Mol. Cell. Neurosci. 80, 44–51. https://doi.org/10.1016/j.mcn.2017.02.003.
Wang, O., Zheng, Z., Wang, Q., Jin, Y., Jin, W., Wang, Y., Chen, E., Zhang, X., 2017. ZCCHC12, a novel oncogene in papillary thyroid cancer. J. Cancer Res. Clin. Oncol. 143, 1679–1686. https://doi.org/10.1007/s00432-017-2414-6.
Xu, Y., Wang, K., Yu, Q., 2016. FRMD6 inhibits human glioblastoma growth and progression by negatively regulating activity of receptor tyrosine kinases. Oncotarget 7, 70080–70091. https://doi.org/10.18632/oncotarget.12148.
Xu, Z., Liang, Q., Song, X., Zhang, Z., Lindtner, S., Li, Z., Wen, Y., Liu, G., Guo, T., Qi, D., Wang, M., Wang, C., Li, H., You, Y., Wang, X., Chen, B., Feng, H., Rubenstein, J.L., Yang, Z., 2018. Sp8 and Sp9 coordinately promote D2-type medium spiny neuron production by activating Six3 expression. Development. https://doi.org/10.1242/dev.165456.
Yun, K., Fischman, S., Johnson, J., Hrabe de Angelis, M., Weinmaster, G., Rubenstein, J.L., 2002. Modulation of the notch signaling by Mash1 and Dlx1/2 regulates sequential specification and differentiation of progenitor cell types in the subcortical telencephalon. Development 129, 5029–5040.
Zhang, Q., Zhang, Y., Wang, C., Xu, Z., Liang, Q., An, L., Li, J., Liu, Z., You, Y., He, M., Mao, Y., Chen, B., Xiong, Z.Q., Rubenstein, J.L., Yang, Z., 2016. The zinc finger transcription factor Sp9 is required for the development of striatopallidal projection neurons. Cell Rep. 16, 1431–1444. https://doi.org/10.1016/j.celrep.2016.06.090.